

# OBSERVATION OF POLARIZATION-DEPENDENT CHANGES IN HIGHER-ORDER MODE RESPONSES AS A FUNCTION OF TRANSVERSE BEAM POSITION IN TESLA-TYPE CAVITIES AT FAST\*

R. M. Thurman-Keup<sup>†</sup>, D. R. Edstrom, A. H. Lumpkin, P. S. Prieto, J. Ruan  
Fermi National Accelerator Laboratory, Batavia, IL, USA  
J. A. Diaz Cruz<sup>1</sup>, B. T. Jacobson, J. P. Sikora, F. Zhou  
SLAC National Accelerator Laboratory, Menlo Park, CA, USA  
<sup>1</sup>also at University of New Mexico, Albuquerque, NM, USA

## Abstract

Higher-order modes (HOMs) in superconducting rf cavities present problems for an electron bunch traversing the cavity in the form of long-range wakefields from previous bunches. These may dilute the emittance of the macropulse average, especially with low emittance beams at facilities such as the European X-ray Free-electron Laser (XFEL) and the upgraded Linac Coherent Light Source (LCLS-II). Here we present observations of HOMs driven by the beam at the Fermilab Accelerator Science and Technology (FAST) facility. The FAST facility features two independent TESLA-type cavities (CC1 and CC2) after a photocathode rf gun followed by an 8-cavity cryomodule. The HOM signals were acquired from cavities using bandpass filters of  $1.75 \pm 0.15$  GHz,  $2.5 \pm 0.2$  GHz, and  $3.25 \pm 0.2$  GHz and recorded using an 8-GHz, 20 GSa/s oscilloscope. The frequency resolution obtained is sufficient to separate polarization components of many of the HOMs. These HOM signals were captured from CC1 and cavities 1 and 8 of the cryomodule for various initial trajectories through the cavities, and we observe correlations between trajectory, HOM signals, and which polarization component of a mode is affected.

## INTRODUCTION

Beam traversing an accelerating cavity can induce higher order mode (HOM) responses in the cavity. These HOMs may impact the beam in the form of long-range wakefields. At high-brightness electron accelerator facilities such as the European XFEL at DESY [1] and LCLS-II at SLAC [2], these wakefields may cause emittance dilution as the beam is transported down the beamline, particularly through the early cryomodules. In this paper, we focus on the dipole modes of TESLA-type 9-cell cavities [3-5] which are generated when the transverse position of the bunch does not align with the electromagnetic center of the mode. The response of the mode is then a linear function of the transverse distance of the bunch from the electromagnetic center. Each dipole mode has two polarizations which are typically split in frequency due to the cavity shape not being exactly cylindrical.

Previous efforts at DESY to reduce these HOM wakefields involved the use of a narrowband, down-converted signal filtered on the TE111-6 dipole mode at  $\sim 1.7$  GHz to measure and correct the beam position through the cavities [6]. Here we look at some of the dipole modes from 1.6 GHz to 1.9 GHz in a stand-alone cavity and in 4 of the cavities of a cryomodule. We have used horizontal and vertical corrector magnets in front of the cavities to steer the beam and produce an average offset through the cavities. These offsets produce varying levels of HOM signals which we process through an oscilloscope to obtain the magnitude and phase of the modes including the two polarizations for some of them. Additionally, we identify modes that are close to beam harmonics which may induce larger effects in the later bunches due to coherent summing of the HOM fields. In the past [7, 8], we have identified modes that caused motion along the bunch train at the difference frequency of the mode and a beam harmonic.

## EXPERIMENTAL SETUP

### Accelerator Infrastructure

The FAST Linac [9] (Fig. 1) consists of a photocathode electron gun with a Cs<sub>2</sub>Te cathode driven by a Nd:YLF laser. The photocathode is embedded in a normal conducting rf cavity operating at 1.3 GHz and surrounded by 2 solenoids. The laser repetition rate is typically 3 MHz and can produce electron bunches from below 100 pC to several nC which exit the gun with  $\sim <5$  MeV of energy. Following the gun are two 9-cell TESLA-type superconducting rf cavities (CC1 and CC2) which together can increase the energy up to 50 MeV. After the cavities is a section with quadrupoles and an optional spectrometer magnet and low energy dump. This section has many diagnostic stations in it, including Al OTR foils, YAG:Ce single-crystal screens, and an Al-coated Si transition radiation screen leading to a THz interferometer and a streak camera for bunch length measurements. Beyond this section is the cryomodule (CM2) containing 8 TESLA-type cavities, followed by the high-energy line ending at the absorber. The cavities all have a higher-order mode (HOM) coupler at each end to couple out the HOMs generated by the passing beam. The horizontal and vertical dipole correctors upstream of the cavities are used to alter the trajectory through the cavities producing varying levels of HOMs. The correctors at location 101 and 125 are used to steer the beam in CC1/CC2 and CM2 respectively.

\* This manuscript has been authored by Fermi Research Alliance, LLC under Contract No. DE-AC02-07CH11359 with the U.S. Department of Energy, Office of Science, Office of High Energy Physics.

<sup>†</sup> keup@fnal.gov

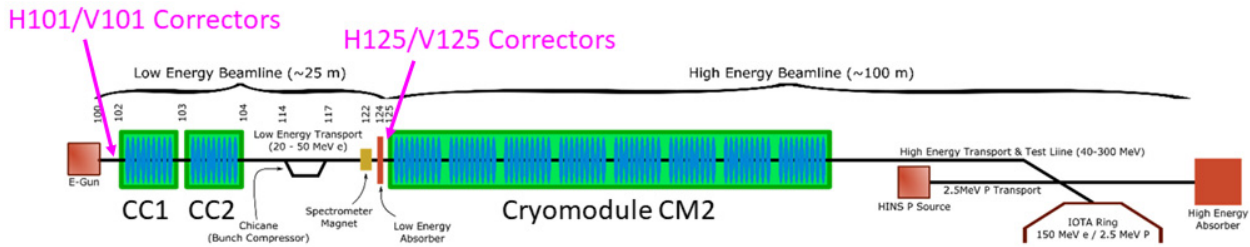


Figure 1: FAST Linac showing the location of the CC1 and CC2 single cavities, and the cryomodule CM2 with 8 cavities. The corrector locations are also shown just upstream of the cavity locations. This schematic is not to scale.

### Instrumentation

The HOM signals are transported from the cavities to the electronics via 1/2" Heliax cables. Once in the rack, they transition to BNC-terminated RG-58 cables for convenience before entering one of several analog filter boxes. Since there were different filter boxes being tested, a patch panel was used to quickly switch between cavities and boxes (Fig. 2).

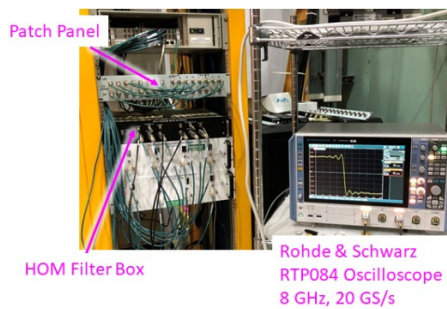


Figure 2: Acquisition system showing the patch panel, the black filter box, and the oscilloscope.

The schematic of the HOM filter box used in this set of measurements is shown in Fig. 3. It contains two channels, with each channel having three bandpass filters at 1.75 GHz, 2.5 GHz, and 3.25 GHz, and an optional 20 dB amplifier controlled by a switch on the front panel. Three of the outputs (one of each frequency band) pass through a Schottky diode to rectify the signal before sending it to a digitizer in the control system. The other three outputs are connected to an 8-GHz analog bandwidth, 20-GS/s, Rohde & Schwarz RTP084 oscilloscope which records the HOM signals for further processing offline. The initial DC block in the circuit is to prevent any charge buildup from getting to the 1.3 GHz notch filter.

### HOM DATA

The measurements in this paper focus on the 1.75 GHz region which contains the first 18 dipole HOM modes. The time domain signal of this region is shown in Fig. 4 along with the spectra of 4 cavities in CM2 where one can see the variation in the mode frequencies. Also shown are the measured mode values using a network analyzer connected between the two couplers of the cavity, and the 3 MHz beam harmonics. Figure 5 shows a specific mode at ~1.73 GHz where the agreement with the network analyzer and proximity to beam harmonics can be more easily seen.

The proximity to the beam harmonics is important when considering build-up of the HOMs along bunch train.

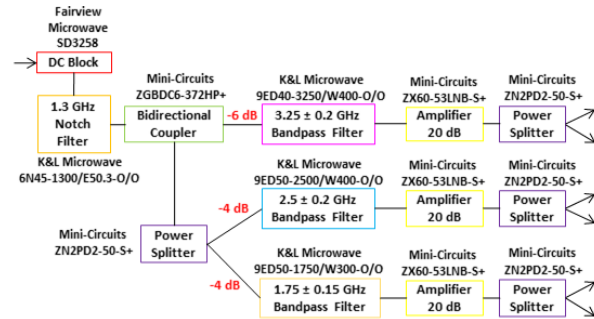


Figure 3: Schematic of the filter circuit. The red dB numbers indicate the relative amplitudes of the three channels after the combined bidirectional coupler and power splitter.

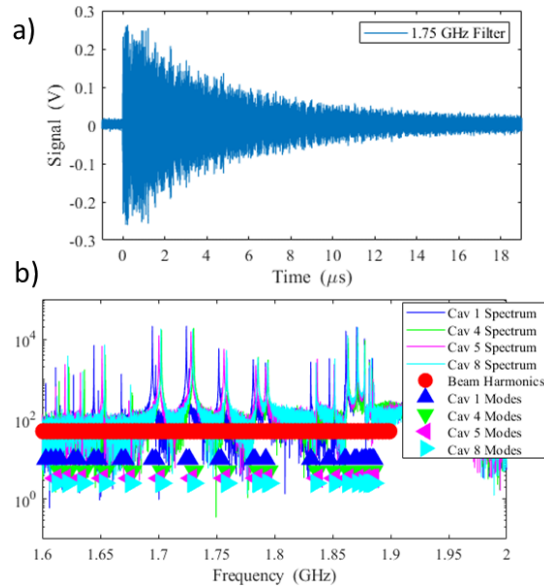


Figure 4: a) HOM signals from cavity 1 of CM2. b) Spectra of 4 cavities in CM2.

To study the effect of HOMs on the beam [10, 11], the beam was steered by the H125/V125 corrector magnets. In Fig. 6, we plot the CM2, cavity 1 HOM spectra of the mode at ~1.75 GHz for various corrector magnet currents. We can see that for this mode, the two polarizations seem to coincide with horizontal and vertical as shown by the fact that only one polarization changes for each steering direction.

Content from this work may be used under the terms of the CC BY 3.0 licence (© 2021). Any distribution of this work must maintain attribution to the author(s), title of the work, publisher, and DOI

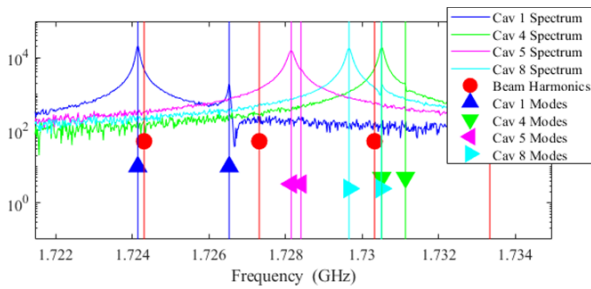


Figure 5: HOM spectra near the ~1.73 GHz mode from 4 cavities of CM2 showing the spread in frequencies among cavities.

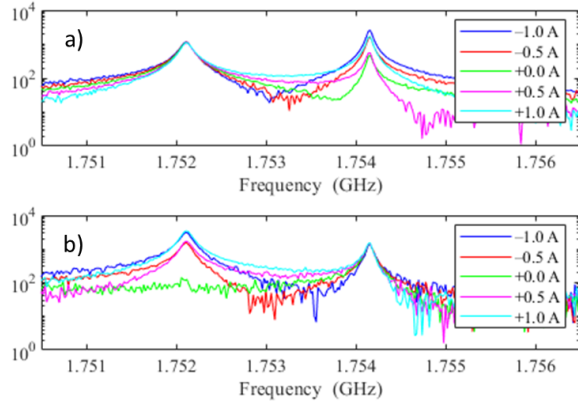


Figure 6: Horizontal a) and vertical b) steering results showing polarization-dependent HOM variations.

To correlate the HOMs with beam steering direction requires the phase of the HOM as well as the magnitude. Extracting the phase requires a stable trigger. For these measurements, we used a trigger for the oscilloscope that is stable enough to allow a time correction to be applied later. Figure 7 shows the start of the HOM signals which should be dominated by the arrival time of the bunch at the HOM pickup. One can see variation in the arrival time which needs to be corrected to get the correct phase of the HOMs. The bottom plot shows the signals after adjusting for the jitter using the peak located at  $t = 0$  ns.

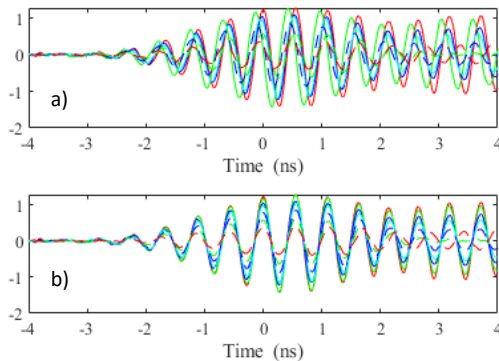


Figure 7: a) HOM signals from oscilloscope. b) After aligning time signals using the peak at 0 ns.

Figure 8 shows the spectra of the ~1.75 GHz mode after aligning the time and plotted as a product of the amplitude and cosine of the phase relative to the phase of the +1 A case. One sees the expected behaviour, where trajectories

on opposite sides of center produce HOMs that are 180 degrees out of phase.

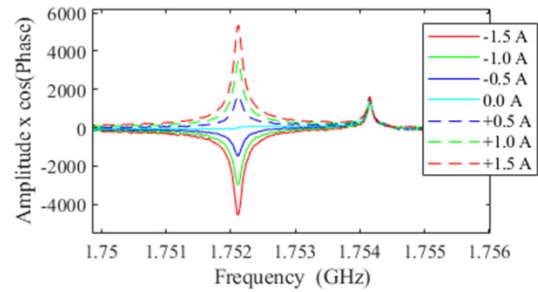


Figure 8: "Signed" spectra of ~1.75 GHz mode.

In Fig. 9, we plot the full magnitude and phase of the peak and adjacent spectral values of the 1.73 GHz mode for cavities 1, 4, 5 and 8 of CM2, for various vertical corrector currents. There is an interesting feature here and in other modes. The phase of cavity 1 is noticeably different from the other cavities. It is not clear what causes this.

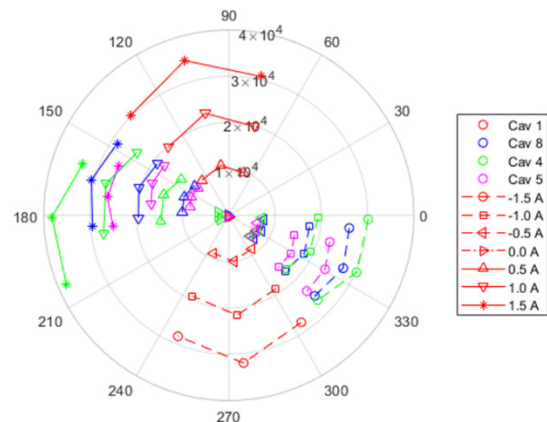


Figure 9: Polar phase plot of ~1.73 GHz HOM mode for various vertical corrector currents.

## CONCLUSION

Using a high bandwidth oscilloscope, we have recorded the dipole HOM signals from TESLA-type 9-cell superconducting rf cavities in an 8-cavity cryomodule and reconstructed the phase and magnitude of certain modes. The reconstruction allows one to ascertain the relative position of the beam with respect to the mode axis. We have used dipole correctors upstream of the cavities to steer the beam and produce a beam offset in the cavity to produce HOMs of varying amplitudes. We have produced changes in particular HOM polarizations dependent on the direction of beam steering. We also find a difference in the phase values in the first cavity of the cryomodule that we don't yet understand.

## ACKNOWLEDGEMENTS

The Fermilab authors acknowledge the support of C. Drennan, A. Valishev, D. Broemmelsiek, G. Stancari, and M. Lindgren, all in the Accelerator Division at Fermilab. The SLAC/NAL authors acknowledge the support of J. Schmerge (Superconducting Linac Division, SLAC).

## REFERENCES

- [1] H. Weise, “Commissioning and First Lasing of the European XFEL”, in *Proc. of 38th Int. Free Electron Laser Conf. (FEL’17)*, Santa Fe, NM, USA, Aug. 2017, pp. 9-13. doi:10.18429/JACoW-FEL2017-MOC03
- [2] P. Emma, “Status of the LCLS-II FEL Project at SLAC”, presented at the 38th Int. Free Electron Laser Conf. (FEL’17), Santa Fe, NM, USA, Aug. 2017, paper MOD01, unpublished.
- [3] B. Aune *et al.*, “Superconducting TESLA cavities”, *Phys. Rev. ST Accel. Beams*, vol. 3, p. 092001, 2000. doi:10.1103/PhysRevSTAB.3.092001
- [4] R. Brinkman *et al.*, “TESLA-Technical Design Report”, DESY, Hamburg, Germany, Rep. DESY-TESLA-2001-23, Part II, 2001.
- [5] R. Wanzenberg, “Monopole, Dipole and Quadrupole Passbands of the TESLA 9-cell Cavity”, DESY, Hamburg, Germany, Rep. DESY-TESLA-2001-33, 2009.
- [6] S. Malloy *et al.*, “High precision superconducting cavity diagnostics with higher order mode measurements”, *Phys. Rev. ST Accel. Beams*, vol. 9, p. 112802, 2006. doi:10.1103/PhysRevSTAB.9.112802
- [7] A. H. Lumpkin *et al.*, “Submacropulse electron-beam dynamics correlated with higher-order modes in Tesla-type superconducting rf cavities”, *Phys. Rev. Accel. Beams*, vol. 21, p. 064401, 2018. doi:10.1103/PhysRevAccelBeams.21.064401
- [8] A. H. Lumpkin, N. Eddy, D. R. Edstrom, J. Ruan, and R. M. Thurman-Keup, “Observations of Long-Range and Short-Range Wakefield Effects on Electron-Beam Dynamics in TESLA-type Superconducting RF Cavities”, in *Proc. 8th Int. Beam Instrumentation Conf. (IBIC’19)*, Malmö, Sweden, Sep. 2019, paper TUPP041, pp. 428-431. doi:10.18429/JACoW-IBIC2019-TUPP041
- [9] S. Antipov *et al.*, “IOTA (Integrable Optics Test Accelerator): Facility and Experimental Beam Physics Program”, *Journal of Instrumentation*, vol. 12, no. 3, p. T03002, May 2017. doi:10.1088/1748-0221/12/03/T03002
- [10] A. H. Lumpkin *et al.*, “Investigations of long-range wakefield effects in a TESLA-type cryomodule at FAST”, presented at the 21th Int. Particle Accelerator Conf. (IPAC’21), Campinas, Brazil, May 2021, paper TUPAB274, this conference.
- [11] J. Sikora *et al.*, “Commissioning of the LCLS-II prototype HOM detectors with TESLA-type cavities at FAST”, presented at the 21th Int. Particle Accelerator Conf. (IPAC’21), Campinas, Brazil, May 2021, paper MOPAB323, this conference.